BAREKENG: Journal of Mathematics and Its Applications
December 2026 Volume 20 Issue 4 Page 2997-3010
P-ISSN: 1978-7227 E-ISSN: 2615-3017
https://doi.org/10.30598/barekengvol20iss4pp2997-3010

COMPARATIVE STUDY ON FREE VERSUS MIXED CONVECTION IN MHD BOUNDARY LAYER FLOW OF VISCOELASTIC MICROPOLAR FLUID OVER A SPHERE

Laila Amera Aziz [1*], Abdul Rahman Mohd Kasim [2], Mohd Zuki Salleh [3], Syazwani Mohd Zokri [4]

[1,2,3] Centre for Mathematical Sciences, Universiti Malaysia Pahang Al-Sultan Abdullah Lebuh Persiaran Tun Khalil Yaakob, Kuantan, Pahang, 26300, Malaysia

[4] Faculty of Computer and Mathematical Sciences, Universiti Teknologi MARA (UiTM) Kampus Kuala Terengganu, 21080, Malaysia

*Corresponding author's e-mail: * **lailaamera@umpsa.edu.my***

Article Info

Article History:

Received: 22nd September 2025
Revised: 27th April 2026
Accepted: 26th May 2026
Available online: 1st July 2026

Keywords:

Keller-Box Method;
Magnetohydrodynamic Convection;
Viscoelastic Micropolar.

ABSTRACT

This study presents a numerical investigation comparing free and mixed convection in boundary layer flow of viscoelastic micropolar fluid over a sphere under magnetohydrodynamic (MHD) effects. A mathematical framework was formulated that consists of the continuity equation, momentum conservation, energy balance, and micropolar constitutive relations. They are expressed as a coupled system of partial differential equations (PDEs). These equations were simplified into ordinary differential equations (ODEs) through similarity transformations and then solved numerically using the Keller-box method in Fortran. The comparative analysis focuses on the distinct characteristics of free and mixed convection regimes, examining the effects of various parameters on skin friction coefficients and heat transfer. Results reveal that viscoelastic and micropolar parameters significantly dictate skin friction and heat transfer, while the magnetic parameter exhibits contrasting impacts depending on the convection regime. Furthermore, boundary layer separation is found to be sensitive to parameter variations only under mixed convection, where increased magnetic and assisting flow effects provide a stabilizing delay. This comparative framework offers a deeper understanding of the fundamental mechanisms governing these convection regimes and their practical implications in engineering applications.

How to cite this article:

L. A. Aziz, A. R. M. Kasim, M. Z. Salleh, and S. M. Zokri, "COMPARATIVE STUDY ON FREE VERSUS MIXED CONVECTION IN MHD BOUNDARY LAYER FLOW OF VISCOELASTIC MICROPOLAR FLUID OVER A SPHERE", *BAREKENG: J. Math. & App.*, vol. 20, no. 4, pp. 2997-3010, Dec. 2026.

Journal homepage: *https://ojs3.unpatti.ac.id/index.php/barekeng/*
Journal e-mail: *barekeng.math@yahoo.com; barekeng.journal@mail.unpatti.ac.id*

Research Article · Open Access

1. INTRODUCTION

Convective transport, the primary mode of heat and mass transfer in fluids, is a fundamental phenomenon observed across numerous scientific and engineering fields. This mechanism helps explain how various processes occur, including atmospheric and oceanic circulation [1], industrial operations [2], as well as biological systems [3]. In engineering, the efficiency of heat exchangers, combustion, and cooling systems relies heavily on convective heat transfer. This is especially important for maintaining the performance of devices such as electronics, power plants, and transportation systems.

Free convection, driven primarily by buoyancy force, plays a vital role in passive cooling. It supports heat transfer in cooling components for electronics and natural building ventilation without requiring external energy. Mixed convection, where buoyancy and forced flow interact, is dominant in processes like industrial drying and advanced electronic component cooling [4]. In chemical processing and materials manufacturing, such as polymer extrusion, metal forming, and crystal growth, understanding these convection modes enables precise temperature control. Engineers exploit free convection for energy-efficient designs and apply mixed convection knowledge to optimize complex systems where both natural and forced flows are present [5]. The ability to predict and control these phenomena directly translates to improvements in energy efficiency, product quality, system reliability, and reduced operating costs across a wide range of industries.

Convection modes and boundary layers are highly associated in fluid dynamics. The boundary layer is the thin region near a surface where rapid changes in fluid velocity significantly affect heat transfer [6]. Free convection creates boundary layers that are thicker and slower due to temperature-driven flow, while forced convection uses external pressure that results in thinner, faster layers with better heat transfer [7]. Mixed convection occurs when these two forces combine, creating a unique flow where both buoyancy and external pressure determine the final boundary layer behavior. Understanding how boundary layers change with different convection types, especially during laminar-to-turbulent transitions, is crucial for designing efficient heating and cooling systems. This provides the rationale for investigating boundary layer flow across various convection modes.

According to [8], the period from 1900 to 1930 marked a milestone in the study of convective heat transfer, leading to major advances in the field. Prandtl's boundary layer theory introduced a transformative perspective to fluid mechanics by distinguishing regions dominated by viscous effects from those governed by inviscid flow [9]. Although not originally focused on convection, this groundbreaking idea laid the foundation for subsequent studies on thermal and velocity boundary layers within convective flow systems. The early studies on convection include [10], whose analysis of linear velocity profiles near walls became essential for developing models of thermal boundary layers in free convection, while [11] developed an approximate method for solving boundary layer momentum equations that enabled simplified analysis of boundary layer flows with heat transfer, which was later adapted for mixed convection problems.

Afterwards, [12] introduced generalized similarity solutions for boundary layers that are applicable to both free and mixed convection, thus emphasizing the interrelation and shared principles between these two modes of convection. Later developments on convective studies then extended these pioneering ideas into various fluid geometries and effects. For instance, [13], [14], and [15] developed the models for free convection boundary layer flow of micropolar fluid on the surface of various geometries, namely the vertical flat plate, isothermal sphere, and cylinder, respectively. Similarly, all these problems utilized the Keller-box method, hence displaying the versatility of the finite difference method across geometries. Besides these studies, the boundary layer flow model for free convection has also been formulated by [16] for nanofluid under aligned MHD effect, while [17] investigates viscoelastic fluid flow with porous condition. The studies indicate that kerosene-based nanofluids improve heat transfer; however, viscoelasticity, in contrast, forms a resistance to the heat transfer process.

A thorough understanding of free convection problems enables a deeper exploration of the more complex mixed convection phenomena. Built upon the previously established free convection model [18] advanced her study by formulating a Brinkman-viscoelastic model for the mixed convection mode. Likewise, [19] also started with a free convection model for micropolar fluid on a solid sphere before publishing their next work on the same problem for mixed convection [20]. Using the Keller-box method to solve both problems, these studies reveal that the existence of microelements in fluid tends to increase skin friction and suppress heat transfer across different modes of convection in Newtonian heating. It has become increasingly common for researchers to study both free and mixed convection boundary layer flows involving diverse fluid models and geometries, as shown in recent studies by [21], [22] focusing on viscoelastic nanofluid flow and [23], [24] that examine the flow of Casson nanofluid. This trend highlights the importance of examining both modes of convection, as it helps us understand and predict heat transfer in real situations where natural and forced flows coexist.

However, despite the prevalence of studies on individual convection modes, comparative analyses between free and mixed convection remain limited in the literature. This includes the problem of viscoelastic micropolar fluid over a sphere, where only the effect of significant parameters on the mixed convection flow has been discussed [25]. Comparative investigations could provide valuable insights for early researchers in boundary layer theory regarding the expected similarities and differences between free and mixed flow models. Furthermore, comparative analyses could guide practitioners in determining whether external flows would enhance processes relevant to their specific applications. Therefore, to address this gap, this study examines the distinctive characteristics of free and mixed convection within magnetohydrodynamic boundary layer flows of viscoelastic micropolar fluids around a sphere, analyzing the interplay between viscoelasticity effects, electromagnetic forces, microrotation effects, and thermal transport mechanisms under varying convection regimes.

2. RESEARCH METHODS

The following figure illustrates the physical coordinate system for the incompressible two-dimensional flow of a viscoelastic micropolar fluid over a sphere. For the free convection case in Fig. 1 (a), the flow is solely buoyancy-driven, whereas the mixed convection case in Fig. 1 (b) includes an external flow U_∞ that is directed vertically upward from the lower stagnation point. This study evaluates both heating and cooling of the sphere surface. These thermal states dictate the sign of the mixed convection parameter λ, allowing for an analysis of both assisting ($\lambda > 0$) and opposing ($\lambda < 0$) flow scenarios.

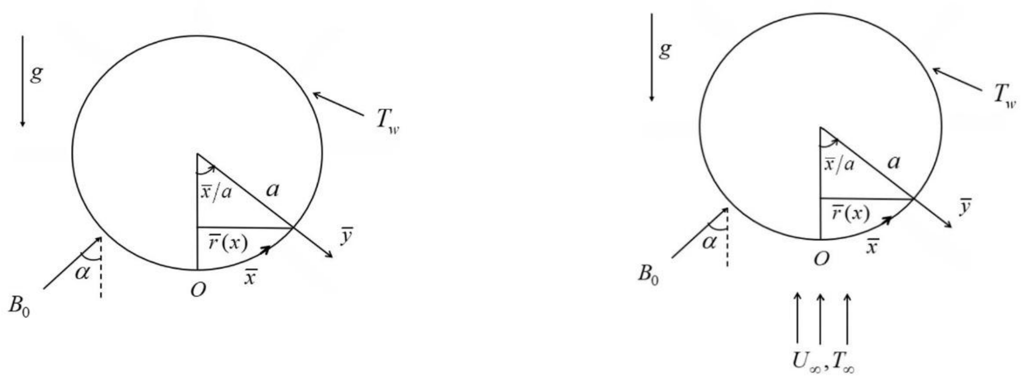

(a) **(b)**

Figure 1. Schematic Diagrams of (a) Free Convection and (b) Mixed Convection Boundary Layer Flow of Viscoelastic Micropolar Fluid Over a Sphere

The flow is governed by a set of equations consisting of continuity, momentum, micropolar, and energy equations, adapted from the foundational micropolar theory of [26] and the boundary layer formulations for spherical geometries established by [27]. While continuity, micropolar, and energy equations remain consistent across both convection modes, the momentum equation varies. The continuity, micropolar, and energy equations are

$$\frac{\partial}{\partial x}(\bar{r}\,\bar{u}) + \frac{\partial}{\partial y}(\bar{r}\,\bar{v}) = 0, \tag{1}$$

$$\rho j\left(\bar{u}\frac{\partial \bar{H}}{\partial \bar{x}} + v\frac{\partial \bar{H}}{\partial \bar{y}}\right) = -\kappa\left(2\bar{H} + \frac{\partial \bar{u}}{\partial \bar{y}}\right) + \gamma\frac{\partial^2 \bar{H}}{\partial \bar{y}^2}, \tag{2}$$

$$u\frac{\partial T}{\partial x} + v\frac{\partial T}{\partial y} = \chi\frac{\partial^2 T}{\partial y^2}. \tag{3}$$

For free convection, the momentum equation and boundary conditions are

$$\bar{u}\frac{\partial\bar{u}}{\partial\bar{x}}+\bar{v}\frac{\partial\bar{u}}{\partial\bar{y}}=\left(\frac{\mu+\kappa}{\rho}\right)\frac{\partial^2\bar{u}}{\partial\bar{y}^2}+\frac{k_0}{\rho}\left[\frac{\partial}{\partial\bar{x}}\left(\bar{u}\frac{\partial^2\bar{u}}{\partial\bar{y}^2}\right)+\bar{v}\frac{\partial^3\bar{u}}{\partial\bar{y}^3}-\frac{\partial\bar{u}}{\partial\bar{y}}\frac{\partial^2\bar{u}}{\partial\bar{x}\partial\bar{y}}\right]$$
$$+g\beta(T-T_\infty)\sin\left(\frac{\bar{x}}{a}\right)+\frac{\kappa}{\rho}\frac{\partial\bar{H}}{\partial\bar{y}}-\frac{\sigma}{\rho}\bar{u}\,B_0^2\sin^2\alpha\,, \tag{4}$$

$$\bar{u}=\bar{v}=0,\ T=T_w,\ \ \bar{H}=-\frac{1}{2}\frac{\partial\bar{u}}{\partial\bar{y}}\ \ \text{on}\ \ \bar{y}=0,$$
$$\bar{u}=0,\ \ \frac{\partial\bar{u}}{\partial\bar{y}}=0,\ \ T=T_\infty,\ \ \bar{H}=0\ \ \text{as}\ \ \bar{y}\to\infty. \tag{5}$$

The momentum equation for mixed convection models includes an additional term, u_e to represent the external velocity, which arises from the combined effects of forced and buoyancy-driven flows. For this problem, the momentum equation and boundary conditions are in the form:

$$\bar{u}\frac{\partial\bar{u}}{\partial\bar{x}}+\bar{v}\frac{\partial\bar{u}}{\partial\bar{y}}=\bar{u}_e\frac{\partial\bar{u}_e}{\partial\bar{x}}+\left(\frac{\mu+\kappa}{\rho}\right)\frac{\partial^2\bar{u}}{\partial\bar{y}^2}+\frac{k_0}{\rho}\left[\frac{\partial}{\partial\bar{x}}\left(\bar{u}\frac{\partial^2\bar{u}}{\partial\bar{y}^2}\right)+\bar{v}\frac{\partial^3\bar{u}}{\partial\bar{y}^3}+\frac{\partial\bar{u}}{\partial\bar{y}}\frac{\partial^2\bar{v}}{\partial\bar{y}^2}\right]$$
$$+g\beta(T-T_\infty)\sin\left(\frac{\bar{x}}{a}\right)+\frac{\kappa}{\rho}\frac{\partial\bar{H}}{\partial\bar{y}}-\frac{\sigma}{\rho}(\bar{u}-\bar{u}_e)B_0^2\sin^2\alpha, \tag{6}$$

$$\bar{u}=\bar{v}=0,\ T=T_w,\ \ \bar{H}=-\frac{1}{2}\frac{\partial\bar{u}}{\partial\bar{y}}\ \ \text{on}\ \ \bar{y}=0,$$
$$\bar{u}=\bar{u}_e(\bar{x}),\ \ \frac{\partial\bar{u}}{\partial\bar{y}}=0,\ \ T=T_\infty,\ \ \bar{H}=0\ \ \text{as}\ \ \bar{y}\to\infty. \tag{7}$$

Utilizing the dimensionless variables as defined by [28] for free convection as well as [29] and [30] for mixed convection, the governing equations are transformed to the following dimensionless form.

$$\frac{\partial}{\partial x}(r\,u)+\frac{\partial}{\partial y}(r\,v)=0, \tag{8}$$

$$u\frac{\partial H}{\partial x}+v\frac{\partial H}{\partial y}=-K_1\left(2H+\frac{\partial u}{\partial y}\right)+\left(1+\frac{K_1}{2}\right)\frac{\partial^2 H}{\partial y^2}, \tag{9}$$

$$u\frac{\partial\theta}{\partial x}+v\frac{\partial\theta}{\partial y}=\frac{1}{\Pr}\frac{\partial^2\theta}{\partial y^2}. \tag{10}$$

Concurrently, the dimensionless momentum equation and boundary conditions for the free convection scenario are

$$u\frac{\partial u}{\partial x}+v\frac{\partial u}{\partial y}=(1+K_1)\frac{\partial^2 u}{\partial y^2}+K\left[\frac{\partial}{\partial x}\left(u\frac{\partial^2 u}{\partial y^2}\right)+v\frac{\partial^3 u}{\partial y^3}-\frac{\partial u}{\partial y}\frac{\partial^2 u}{\partial x\partial y}\right]$$
$$+\theta\sin x+K_1\frac{\partial H}{\partial y}-Mu\sin^2\alpha, \tag{11}$$

$$u=v=0,\ \theta=1,\ H=-\frac{1}{2}\frac{\partial u}{\partial y}\ \ \text{on}\ \ y=0,$$
$$u=0,\ \ \frac{\partial u}{\partial y}=0,\ \theta=0,\ H=0\ \ \text{as}\ \ y\to\infty. \tag{12}$$

While for mixed convection, the respective equations are as follows.

$$u\frac{\partial u}{\partial x}+v\frac{\partial u}{\partial y}=u_e\frac{\partial u_e}{\partial x}+(1+K_1)\frac{\partial^2 u}{\partial y^2}+K\left[\frac{\partial}{\partial x}\left(u\frac{\partial^2 u}{\partial y^2}\right)+v\frac{\partial^3 u}{\partial y^3}+\frac{\partial u}{\partial y}\frac{\partial^2 v}{\partial y^2}\right]$$
$$+\lambda\theta\sin x+K_1\frac{\partial H}{\partial y}-M(u-u_e)\sin^2\alpha, \tag{13}$$

$$u = v = 0, \ \ \theta = 1, \ H = -\frac{1}{2}\frac{\partial u}{\partial y} \ \text{ on } \ y = 0,$$
$$u_e = \frac{3}{2}\sin x, \quad \frac{\partial u}{\partial y} = 0, \ \ \theta = 0, \ \ H = 0 \ \text{ as } \ y \to \infty. \tag{14}$$

The main parameters in the governing equations that capture the main characteristics of the flow are the viscoelastic parameter, K, the micropolar parameter, K_1, the magnetic parameter, M, and ultimately, the mixed convection parameter, λ. While according to [28] and [29], the parameter $K_1 = \frac{\kappa}{\mu}$ retains the same definition for both free and mixed convection modes, the definitions of K and M differ. For free convection, the parameters are defined as

$$K = \frac{k_0 Gr^{1/2}}{a^2 \rho}, \quad M = \frac{\sigma B_0^2 a^2}{\rho Gr^{1/2} \nu}. \tag{15}$$

Nonetheless, for mixed convection, the same parameters are defined as follows, in addition to the mixed convection parameter.

$$K = \frac{k_0 U_\infty}{a \rho \nu}, \quad M = \frac{\sigma B_0^2 a}{\rho U_\infty}, \quad \lambda = \frac{Gr}{\mathrm{Re}^2} \tag{16}$$

where $Gr = \frac{g\beta(T_w - T_\infty)a^3}{\nu^2}$ and $\mathrm{Re} = \frac{U_\infty a}{\nu}$. For the mixed convection parameter, $\lambda < 0$ represents opposing flow where buoyancy acts against the externally imposed flow, while $\lambda > 0$ is the assisting flow when buoyancy effect increasingly influences the main flow pattern [31]. The other variables followed the definition in [25].

Subsequently, the following identical non-similarity variables as proposed by [32] are utilised for both cases

$$\psi = x r(x) f(x, y), \quad H = x h(x, y), \quad \theta = \theta(x, y) \tag{17}$$

where the stream function, ψ is defined as

$$u = \frac{1}{r}\frac{\partial \psi}{\partial y}, \quad v = -\frac{1}{r}\frac{\partial \psi}{\partial x}. \tag{18}$$

The non-similarity variables inherently satisfy the continuity equation, while the angular momentum and energy equations are transformed to:

$$\left(1 + \frac{K_1}{2}\right)\frac{\partial^2 h}{\partial y^2} + \left(1 + x\frac{\cos x}{\sin x}\right) f \frac{\partial h}{\partial y} - \frac{\partial f}{\partial y} h - K_1\left(2h + \frac{\partial^2 f}{\partial y^2}\right) = x\left(\frac{\partial f}{\partial y}\frac{\partial h}{\partial x} - \frac{\partial f}{\partial x}\frac{\partial h}{\partial y}\right), \tag{19}$$

$$\frac{1}{\Pr}\frac{\partial^2 \theta}{\partial y^2} + \left(1 + x\frac{\cos x}{\sin x}\right) f \frac{\partial \theta}{\partial y} = x\left(\frac{\partial f}{\partial y}\frac{\partial \theta}{\partial x} - \frac{\partial f}{\partial x}\frac{\partial \theta}{\partial y}\right). \tag{20}$$

Meanwhile, the momentum equation and boundary conditions for the free convection case are

$$\begin{aligned}(1 + K_1)\frac{\partial^3 f}{\partial y^3} - \left(\frac{\partial f}{\partial y}\right)^2 + \left(1 + x\frac{\cos x}{\sin x}\right) f \frac{\partial^2 f}{\partial y^2} + \theta\frac{\sin x}{x} + K_1\frac{\partial h}{\partial y} - M\frac{\partial f}{\partial y}\sin^2\alpha \\ + K\left[2\frac{\partial f}{\partial y}\frac{\partial^3 f}{\partial y^3} - \left(1 + x\frac{\cos x}{\sin x}\right)\left(f\frac{\partial^4 f}{\partial y^4} + \left(\frac{\partial^2 f}{\partial y^2}\right)^2\right)\right] \\ = Kx\left[\frac{\partial f}{\partial x}\frac{\partial^4 f}{\partial y^4} - \frac{\partial^2 f}{\partial x \partial y}\frac{\partial^3 f}{\partial y^3} - \frac{\partial f}{\partial y}\frac{\partial^4 f}{\partial x \partial y^3} + \frac{\partial^2 f}{\partial y^2}\frac{\partial^3 f}{\partial x \partial y^2}\right] + x\left(\frac{\partial f}{\partial y}\frac{\partial^2 f}{\partial x \partial y} - \frac{\partial f}{\partial x}\frac{\partial^2 f}{\partial y^2}\right),\end{aligned} \tag{21}$$

$$f = f' = 0, \ \ \theta = 1, \ h = -\frac{1}{2}f'' \ \text{ on } \ y = 0,$$
$$f' = 0, \ \ f'' = 0, \ \ \theta = 0, \ \ h = 0 \ \text{ as } \ y \to \infty. \tag{22}$$

As for the mixed convection scenario, the momentum equation is

$$\begin{aligned}&(1+K_1)\frac{\partial^3 f}{\partial y^3}-\left(\frac{\partial f}{\partial y}\right)^2+\frac{9}{4}\frac{\sin x}{x}\cos x+\lambda\frac{\sin x}{x}\theta+K_1\frac{\partial h}{\partial y}-M\left(\frac{\partial f}{\partial y}-\frac{3}{2}\frac{\sin x}{x}\right)\sin^2\alpha\\&+\left(1+\frac{x}{\sin x}\cos x\right)f\frac{\partial^2 f}{\partial y^2}+K\left[2\frac{\partial f}{\partial y}\frac{\partial^3 f}{\partial y^3}-\left(1+\frac{x}{\sin x}\cos x\right)\left(f\frac{\partial^4 f}{\partial y^4}+\left(\frac{\partial^2 f}{\partial y^2}\right)^2\right)\right]\\&=x\left(\frac{\partial f}{\partial y}\frac{\partial^2 f}{\partial x\partial y}-\frac{\partial f}{\partial x}\frac{\partial^2 f}{\partial y^2}\right)-Kx\left(\frac{\partial f}{\partial x}\frac{\partial^4 f}{\partial y^4}-\frac{\partial^3 f}{\partial y^3}\frac{\partial^2 f}{\partial x\partial y}-\frac{\partial f}{\partial y}\frac{\partial^4 f}{\partial x\partial y^3}+\frac{\partial^2 f}{\partial y^2}\frac{\partial^3 f}{\partial x\partial y^2}\right)\end{aligned}\tag{23}$$

subjected to the boundary conditions

$$\begin{aligned}&f(0)=f'(0)=0,\ \ \theta(0)=1,\ \ h(0)=-\frac{1}{2}f''(0),\\&f'=\frac{3}{2}\frac{\sin x}{x},\ \ f''=0,\ \ \theta=0,\ \ h=0\quad \text{as } y\to\infty.\end{aligned}\tag{24}$$

Considering only the behaviour of the flow in proximity to the lower stagnation point, where $x \approx 0$, Eqs. (19) to (24) are translated to the following ordinary differential equations (ODEs).

$$\left(1+\frac{K_1}{2}\right)h''+2fh'-f'h-K_1(2h+f'')=0,\tag{25}$$

$$\frac{1}{\Pr}\theta''+2f\theta'=0.\tag{26}$$

The momentum equation for the free convection mode is

$$(1+K_1)f'''-f'^2+2ff''+\theta+K_1h'-Mf'\sin^2\alpha+2K\left(f'f'''-ff^{iv}-f''^2\right)=0\tag{27}$$

and the boundary conditions remain as in Eq. (22). As for the mixed convection, the momentum equation with the respective boundary conditions is in the form:

$$(1+K_1)f'''-f'^2+\frac{9}{4}+\lambda\theta+K_1h-M\left(f'-\frac{3}{2}\right)\sin^2\alpha+2ff''+2K\left(f'f'''-ff^{iv}-f''^2\right)=0,\tag{28}$$

$$\begin{aligned}&f(0)=f'(0)=0,\ \ \theta(0)=1,\ \ h(0)=-\frac{1}{2}f''(0),\\&f'=\frac{3}{2},\ \ f''=0,\ \ \theta=0,\ \ h=0\quad \text{as } y\to\infty.\end{aligned}\tag{29}$$

Following [29] and [14], the local skin friction coefficient, C_f and local wall heat transfer coefficient, Q_w for both convection modes are defined as

$$C_f=\left(1+\frac{K_1}{2}\right)xf''(x,0),\quad Q_w=-\theta'(x,0).\tag{30}$$

3. RESULTS AND DISCUSSION

The ODEs in Eqs. (25) to (28), subject to the boundary condition in Eqs. (22) and (29) were solved numerically using the Keller-box method implemented in Fortran. The Keller-box method was selected due to its inherent stability and second-order accuracy, which are essential for capturing the nonsimilar boundary layer development over a sphere. This computational approach yielded results that provide physical insights into the influence of the main parameters $K, K_1, M,$ and λ.

The numerical solution was generated starting from the sphere's front stagnation point and progressed around the sphere until boundary layer separation occurred. For free convection, validation of the results was achieved by comparing them with other micropolar fluid models published by [28] and [14], as demonstrated in Table 1. As for the mixed convection case, the results were authenticated by comparing them with limiting case solutions of the viscous and ferrofluid model in accordance with the results of [33] and [34], as displayed in Table 2. Both tables showed that the numerical solutions obtained display consistency that indicates the reliability of the present models. Even though the parameters were reduced to match limiting cases, the underlying numerical architecture of the viscoelastic micropolar model remains more complex than a standard viscous or ferrofluid model since it solves a larger system of equations. This leads to slight variations in rounding and truncation errors that explain the numerical discrepancy between the models.

Table 1. Values of Q_w at Various x for $K_1 = 1$ and $K_1 = 2$ when Pr $= 0.7$

x	$K_1 = 1$			$K_1 = 2$		
	[28]	[14]	**Present**	[28]	[14]	**Present**
0°	0.4166	0.4165	0.4309	0.3927	0.393	0.4114
10°	0.4156	0.4154	0.4299	0.3917	0.3921	0.4105
20°	0.4128	0.4126	0.4270	0.3891	0.3894	0.4077
30°	0.408	0.4078	0.4215	0.3847	0.385	0.4024
40°	0.4014	0.4014	0.4152	0.3786	0.3789	0.3964
50°	0.3928	0.3925	0.4063	0.3705	0.3709	0.3879
60°	0.3822	0.3818	0.3952	0.361	0.3611	0.3773
70°	0.3696	0.3695	0.3824	0.3491	0.3493	0.3652
80°	0.3547	0.3545	0.3669	0.3353	0.3355	0.3504
90°	0.3374	0.3369	0.3489	0.3192	0.3195	0.3332
100°	-	-	0.3282	-	-	0.3136
110°	-	-	0.3045	-	-	0.2911
120°	-	-	0.2775	-	-	0.2655

Table 2. Comparison values of $-\theta'(x)$ with previous published results for various x and λ at $K = K_1 = M = 0$ and Pr $= 0.7$

x	[33]			[34]			**Present**		
	-1	**0**	**1**	**-1**	**0**	**1**	**-1**	**0**	**1**
0°	0.786	0.815	0.841	0.786	0.815	0.841	0.782	0.816	0.841
10°	0.781	0.810	0.836	0.781	0.810	0.836	0.782	0.811	0.837
30°	0.742	0.774	0.802	0.742	0.774	0.802	0.743	0.775	0.803
50°	0.662	0.703	0.735	0.664	0.704	0.736	0.663	0.703	0.735
70°	0.536	0.595	0.635	0.535	0.594	0.636	0.534	0.594	0.635
90°	-	0.441	0.507	-	0.441	0.507	-	0.440	0.509
100°	-	0.329	0.431	-	0.324	0.431	-	0.326	0.430

Furthermore, the following figures summarise the isolated effect of each parameter when other parameters are held constant, that provide compelling evidence of how convection mode fundamentally alters fluid behavior. When comparing free and mixed convection regimes, we observe both consistent patterns and striking reversals in how key parameters affect the flow dynamics. From the result, both K and K_1 parameters have the same effect in free and mixed convection regimes, where higher viscoelasticity tends to decrease the heat transfer and skin friction coefficient, as shown in Fig. 2 to Fig. 5. The similar effects across the convection modes can be explained by their fundamental material property influences. Larger K enhances the fluid's memory effect and elastic response to stress, creating resistance to deformation that restricts both momentum and heat transfer regardless of flow regime.

In addition, higher K_1 demonstrates stronger coupling between the angular momentum of particles and the fluid's overall momentum. Thus, fluid particles near the surface experience stronger rotational effects, which create additional resistance against the surface, effectively increasing the wall shear stress and energy dissipation through particle rotation. This could interfere with the efficient transfer of heat from the surface to the fluid and lead to a decrease in heat transfer efficiency in both convection modes.

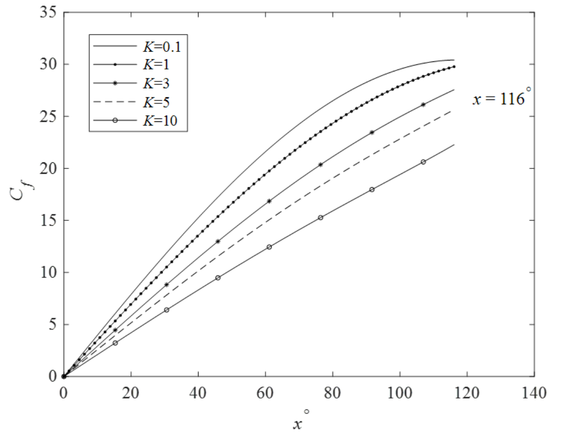

Figure 2. Variation of C_f for Various K at $K_1 = M = 0.5$ and $\alpha = \frac{\pi}{6}$

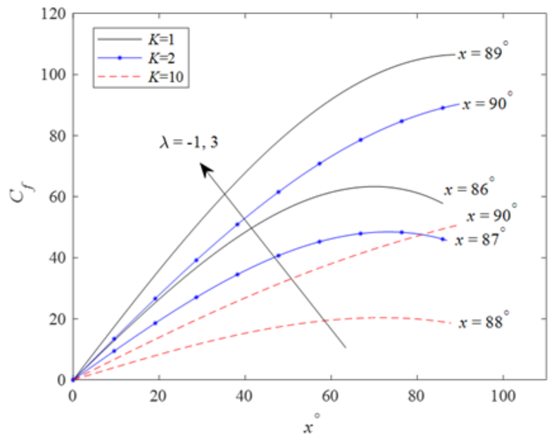

Figure 3. Variation of C_f for Various K and λ at $K_1 = M = 0.5$ and $\alpha = \frac{\pi}{6}$

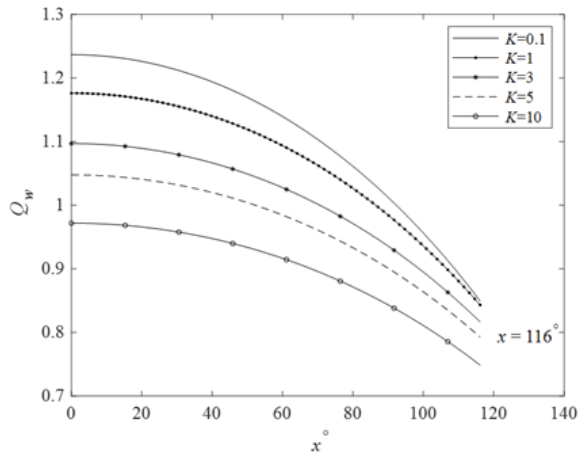

Figure 4. Variation of Q_w for Various K at $K_1 = M = 0.5$ and $\alpha = \frac{\pi}{6}$

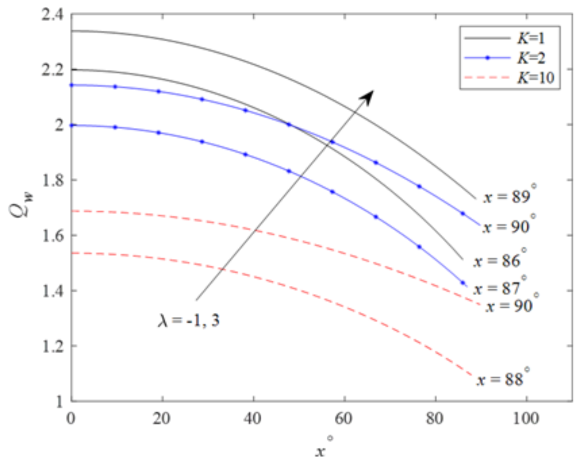

Figure 5. Variation of Q_w for Various K and λ at $K_1 = M = 0.5$ and $\alpha = \frac{\pi}{6}$

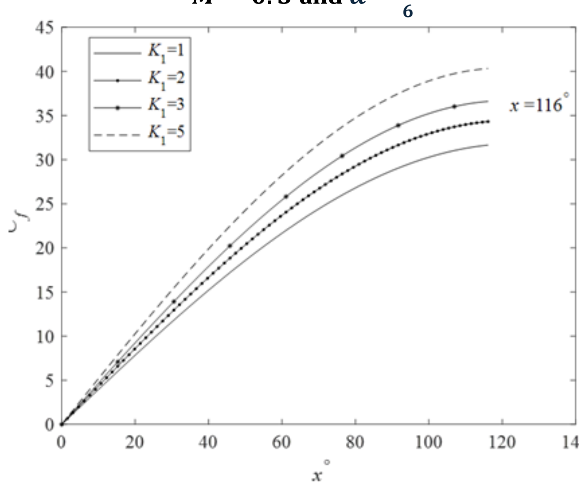

Figure 6. Variation of C_f for Various K_1 at $K = M = 0.5$ and $\alpha = \frac{\pi}{6}$

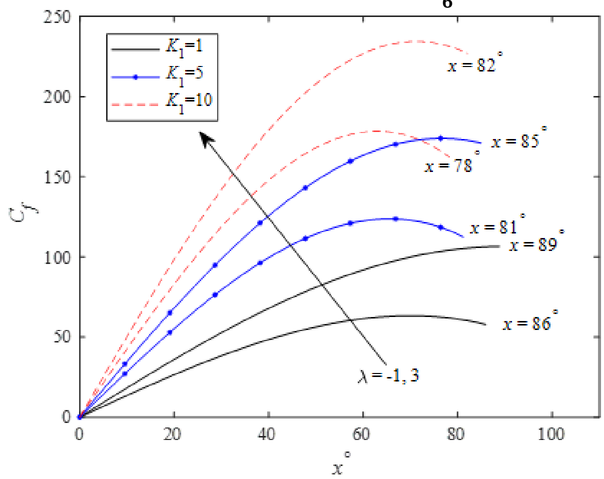

Figure 7. Variation of C_f for Various K_1 and λ at $K = M = 0.5$ and $\alpha = \frac{\pi}{6}$

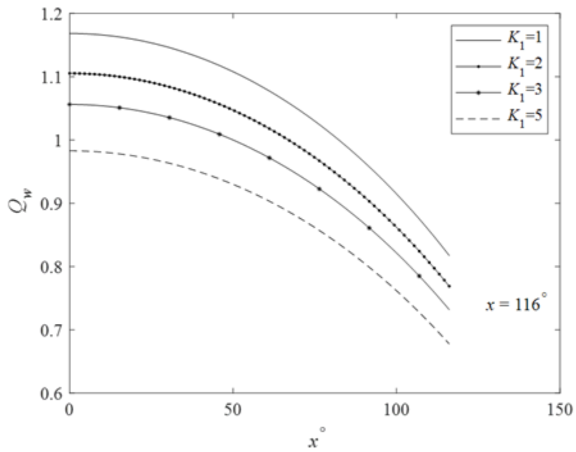

Figure 8. Variation of Q_w for Various K_1 at $K = M = 0.5$ and $\alpha = \frac{\pi}{6}$

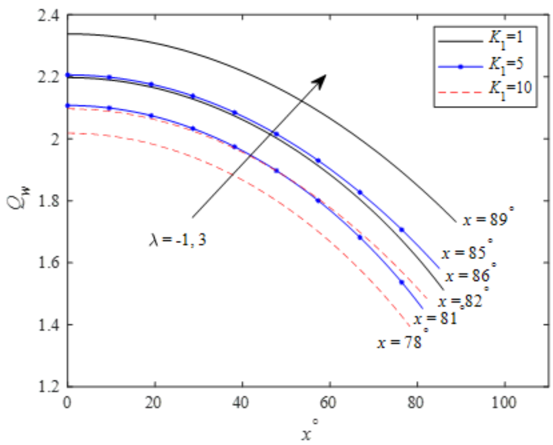

Figure 9. Variation of Q_w for Various K_1 and λ at $K = M = 0.5$ and $\alpha = \frac{\pi}{6}$

On the contrary, an enhancing effect is observed in Fig. 10 to Fig. 13 due to the influence of the magnetic field and inclination angle. This is consistent across both convection regimes, as the skin friction and heat transfer rates increase with higher values of M and α, counteracting the reduction caused by the other two parameters. From the result, M and α behave differently depending on whether the flow is driven by buoyancy or external forces. In free convection, the magnetic field creates a Lorentz force that directly opposes this buoyancy-driven flow, reducing both skin friction and heat transfer. However, in mixed convection, magnetic fields interact with the combined buoyancy-forced flow to enhance momentum and thermal transport.

The results, as illustrated in Fig. 4, Fig. 6, Fig. 8, Fig. 10, and Fig.12, conclusively demonstrate that in free convection mode, the boundary layer separation is robust to the parameter change and the flow remains intact until further back of the sphere at $x = 116^\circ$. In contrast, for mixed convection, as seen in Fig. 3, Fig. 5, Fig. 7, Fig. 9, Fig. 11, and Fig. 13, the separation occurs in advance for higher K and K_1, but it is delayed when M gets larger. This observation is consistent with the results from [28] and [29] that while boundary layer separation is fixed for free convection, it can be controlled in mixed convection by adjusting the balance between buoyancy and external flow. Additionally, Fig. 3 and Fig. 5 also demonstrate that when K varies and λ changes from -1 to 3, the separation point moves from approximately 86° to 89° or 90°. This indicates that increasing λ delays separation, allowing the flow to remain attached to the sphere surface for a longer distance. For the mixed convection parameter, $\lambda < 0$ represents opposing flow where buoyancy acts against the externally imposed flow, while $\lambda > 0$ is the assisting flow when buoyancy effect increasingly influences the main flow pattern [31]. Similar results can be observed as K_1 and M vary when the flow shifts from opposing to assisting flow in Fig. 7, Fig. 9, Fig. 11, and Fig. 13.

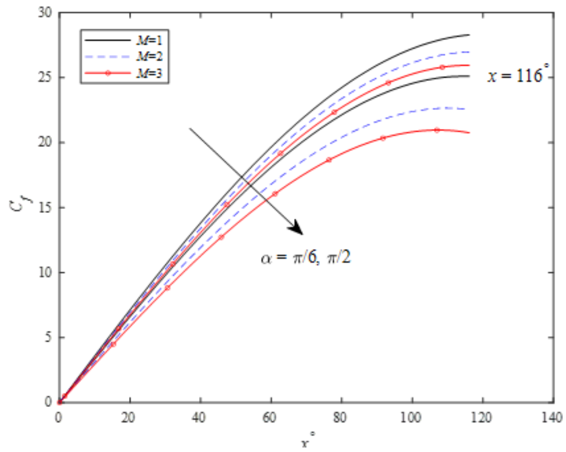

Figure 10. Variation of C_f for Various M at $K = K_1 = 0.5$ and $\alpha = \frac{\pi}{6}$

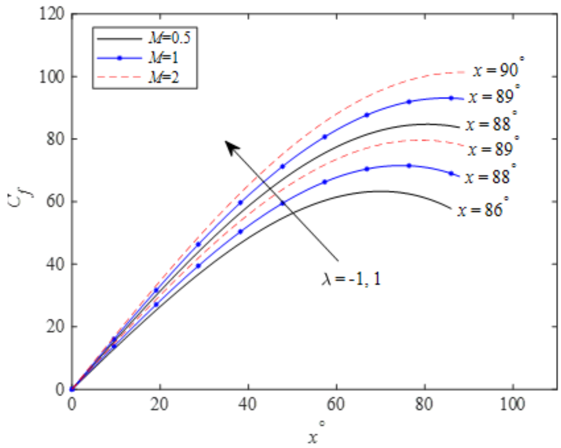

Figure 11. Variation of C_f for Various M and λ at $K = K_1 = 0.5$ and $\alpha = \frac{\pi}{6}$

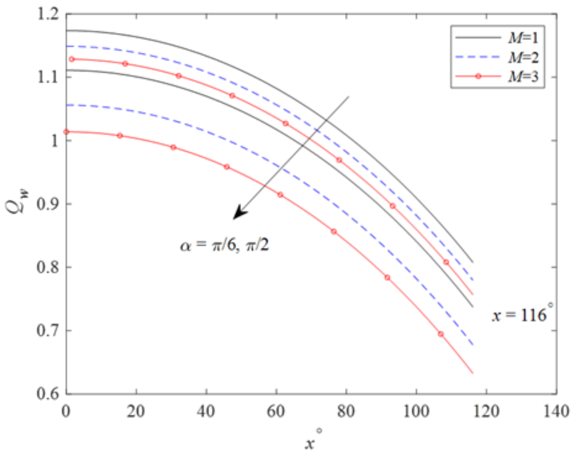

Figure 12. Variation of Q_w for Various M at $K = K_1 = 0.5$ and $\alpha = \frac{\pi}{6}$

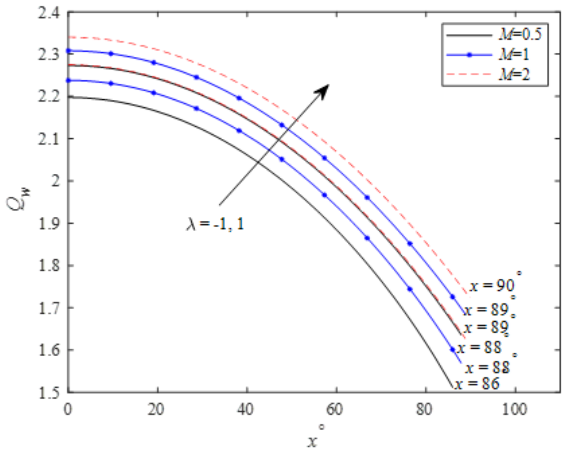

Figure 13. Variation of Q_w for Various M and λ at $K = K_1 = 0.5$ and $\alpha = \frac{\pi}{6}$

4. CONCLUSION

This study investigates the comparative effects of free and mixed convection on the boundary layer flow of viscoelastic micropolar fluid over a sphere with aligned MHD effects. By systematically varying the viscoelasticity, micropolar, and magnetic parameters and examining different mixed convection scenarios, the research reveals significant differences in flow behavior between the two convection regimes. The findings demonstrate how these parameters influence skin friction coefficient, heat transfer rates, and boundary layer separation points, highlighting both consistent patterns and notable reversals in parameter effects across convection modes. The comparative analysis reveals that the transition from free to mixed convection fundamentally changes how the fluid reacts to electromagnetic and microstructure forces. In purely buoyancy-driven or free flow, the point where the fluid layer separates from the sphere remains stable and predictable. In contrast, the addition of an external pressure gradient in mixed convection creates a regime where magnetic and viscoelastic factors can significantly move this separation point.

The difference in flow structure has a direct impact on surface performance. Although both modes respond to parameter changes, the effects on skin friction and heat transfer are far more pronounced in the mixed convection regime due to its higher sensitivity. Remarkably, the magnetic parameter acts as a decelerator in free convection but serves as a flow stabilizer in mixed convection. This demonstrates that the final impact of MHD effects is not universal but rather depends on which convection mode is dominant. The summary of the findings is listed below.

1. Higher K consistently decreases C_f and Q_w for free and mixed convection.
2. Regardless of the convection mode, larger K_1 decreases the heat transfer but increases the skin friction coefficient.

3. M shows opposite impacts between convection modes, where both physical quantities decline in free convection as M grows, while the contrary is observed in mixed convection.
4. Increasing λ (from opposing to assisting flow) enhances both C_f and Q_w.
5. Separation remains consistent regardless of parameter changes in free convection.
6. However, in mixed convection, higher K and K_1 advance separation, while greater M and λ delay separation.

While these results provide clear insights, they are based on the specific assumptions of a steady, two-dimensional, and incompressible flow model. Therefore, the findings may vary under different physical conditions. Future research could expand on this work by considering variable fluid properties or the effects of thermal radiation to better represent complex real-world engineering systems.

Author Contributions

Laila Amera Aziz: Conceptualization, Methodology, Writing-Original Draft, Software, Validation. Abdul Rahman Mohd Kasim: Formulation, Supervision, Validation, Resources. Mohd Zuki Salleh: Formal Analysis, Validation. Syazwani Mohd Zokri: Visualization, Editing. All authors discussed the results and contributed to the final manuscript.

Funding Statement

The authors would like to acknowledge with gratitude the funding support from Tabung Persidangan Dalam Negara (TPDN), Universiti Malaysia Pahang Al-Sultan Abdullah.

Acknowledgment

The authors would like to express their gratitude and appreciation to all parties who have supported and contributed to this research.

Declarations

The authors confirm that has no conflicts of interest to report on this study.

Declaration of Generative AI and AI-assisted Technologies

Generative AI tools (e.g., ChatGPT) were used solely for language refinement, including grammar, spelling, and clarity. The scientific content, analysis, interpretation, and conclusions were developed entirely by the authors. All final text was reviewed and approved by the authors.

REFERENCES

[1] H. A. Nabwey, M. Ashraf, and A. Rashad, "A COMPREHENSIVE REVIEW OF CONVECTIVE HEAT TRANSFER IN HUMID AIR AND ITS PHYSICAL PERSPECTIVES IN CLIMATE CHANGE," *AIP Advances*, vol. 15, no. 5, 2025, doi: https://doi.org/10.1063/5.0270951.

[2] Y. Huang, J. Ge, Y. Chen, and C. Zhang, "NATURAL AND FORCED CONVECTION HEAT TRANSFER CHARACTERISTICS OF SINGLE-PHASE IMMERSION COOLING SYSTEMS FOR DATA CENTERS," *International Journal of Heat and Mass Transfer*, vol. 207, p. 124023, 2023, doi: https://doi.org/10.1016/j.ijheatmasstransfer.2023.124023.

[3] E. Salzer, Z. Gorgin Karaji, M. van Doeselaar, M. A. Tryfonidou, and K. Ito, "THE ROLE OF LOADING-INDUCED CONVECTION VERSUS DIFFUSION ON THE TRANSPORT OF SMALL MOLECULES INTO THE INTERVERTEBRAL DISC," (in eng), *Eur Spine J*, vol. 34, no. 1, pp. 326-337, Jan 2025, doi: https://doi.org/10.1007/s00586-024-08589-9.

[4] R. Henniche and A. Korichi, "MIXED AND FORCED CONVECTION HEAT TRANSFER IN BAFFLED CHANNELS: A BRIEF REVIEW," *Journal of Heat and Mass Transfer Research*, vol. 12, no. 1, pp. 15-28, 2025, doi: https://doi.org/10.22075/JHMTR.2024.34280.1565.

[5] W. Sun *et al.*, "STUDY ON INTERACTION MECHANISM BETWEEN NATURAL CONVECTION AND FORCED CONVECTION DURING STORAGE AND TEMPERATURE RISE OF WAXY CRUDE OIL TANK," *Engineering Applications of Computational Fluid Mechanics*, vol. 19, no. 1, p. 2498354, 2025, doi: https://doi.org/10.1080/19942060.2025.2498354.

[6] T. L. Bergman and A. S. Lavine, *FUNDAMENTALS OF HEAT AND MASS TRANSFER*. 8 ED. HOBOKEN, NJ: John Wiley & Sons, 2017.

[7] Y. Cengel and A. J. Ghajar, *HEAT AND MASS TRANSFER: FUNDAMENTALS AND APPLICATIONS*. MCGRAW-HILL EDUCATION, 2020.

[8] E. R. G. Eckert, "A PIONEERING ERA IN CONVECTIVE HEAT TRANSFER RESEARCH," *in International Heat Transfer Conference Digital Library*, pp. 1-8, Sept. 6-10, 1982.doi:http://dx.doi.org/10.1615/IHTC7.4180.

[9] J. D. Anderson, "LUDWIG PRANDTL'S BOUNDARY LAYER," *Physics Today*, vol. 58, no. 12, pp. 42-48, 2005, doi: https://doi.org/10.1063/1.2169443.

[10] A. Lévêque, "LES LOIS DE LA TRANSMISSION DE CHALEUR PAR CONVECTION," *Annales des Mines*, vol. 13, pp. 201–299, 1930.

[11] E. Pohlhausen, "DER WÄRMEAUSTAUSCH ZWISCHEN FESTEN KÖRPERN UND FLÜSSIGKEITEN MIT KLEINER REIBUNG UND KLEINER WÄRMELEITUNG," *ZAMM-Journal of Applied Mathematics and Mechanics/Zeitschrift für Angewandte Mathematik und Mechanik*, vol. 1, no. 2, pp. 115-121, 1921, doi: https://doi.org/10.1002/zamm.19210010205.

[12] V. M. Falkner, "SOLUTIONS OF THE BOUNDARY LAYER EQUATIONS," *The London, Edinburgh, and Dublin Philosophical Magazine and Journal of Science*, vol. 12, pp. 865-896, 1931, doi: https://doi.org/10.1080/14786443109461870.

[13] D. A. S. Rees and I. Pop, "FREE CONVECTION BOUNDARY-LAYER FLOW OF A MICROPOLAR FLUID FROM A VERTICAL FLAT PLATE," *IMA Journal of Applied Mathematics*, vol. 61, no. 2, pp. 179-197, 1998, doi: https://doi.org/10.1093/imamat/61.2.179.

[14] O. A. Bég, V. R. Prasad, B. Vasu, N. B. Reddy, Q. Li, and R. Bhargava, "FREE CONVECTION HEAT AND MASS TRANSFER FROM AN ISOTHERMAL SPHERE TO A MICROPOLAR REGIME WITH SORET/DUFOUR EFFECTS," *International Journal of Heat and Mass Transfer*, vol. 54, no. 1-3, pp. 9-18, 2011, doi: https://doi.org/10.1016/j.ijheatmasstransfer.2010.10.005.

[15] T. Tayebi, A. Dogonchi, A. J. Chamkha, M. B. B. Hamida, S. El-Sapa, and A. M. Galal, "MICROPOLAR NANOFLUID THERMAL FREE CONVECTION AND ENTROPY GENERATION THROUGH AN INCLINED I-SHAPED ENCLOSURE WITH TWO HOT CYLINDERS," *Case Studies in Thermal Engineering*, vol. 31, 2022, doi: https://doi.org/10.1016/j.csite.2022.101813.

[16] N. A. Rosaidi, N. H. Ab Raji, S. N. H. A. Ibrahim, and M. R. Ilias, "ALIGNED MAGNETOHYDRODYNAMICS FREE CONVECTION FLOW OF MAGNETIC NANOFLUID OVER A MOVING VERTICAL PLATE WITH CONVECTIVE BOUNDARY CONDITION," *Journal of Advanced Research in Fluid Mechanics and Thermal Sciences*, vol. 93, no. 2, pp. 37-49, 2022, doi: https://doi.org/10.37934/arfmts.93.2.3749.

[17] S. F. H. Mohd Kanafiah, A. R. M. Kasim, S. M. Zokri, N. S. Arifin, N. S. Nordin, and M. a. Mokhtar, "FREE CONVECTION BOUNDARY LAYER FLOW OF BRINKMAN-VISCOELASTIC FLUID OVER A HORIZONTAL CIRCULAR CYLINDER WITH CONSTANT WALL TEMPERATURE," *CFD Letters*, vol. 15, pp. 103-114, 2023, doi: https://doi.org/10.37934/cfdl.15.1.103114.

[18] S. F. H. M. Kanafiah, A. R. M. Kasim, S. M. Zokri, and M. R. Ilias, "COMBINED CONVECTIVE TRANSPORT OF BRINKMAN-VISCOELASTIC FLUID ACROSS HORIZONTAL CIRCULAR CYLINDER WITH CONVECTIVE BOUNDARY CONDITION," *Journal of Advanced Research in Fluid Mechanics and Thermal Sciences*, vol. 89, no. 2, pp. 15-24, 2022, doi: https://doi.org/10.37934/arfmts.89.2.1524.

[19] M. Salleh, R. Nazar, and I. Pop, "MODELING OF FREE CONVECTION BOUNDARY LAYER FLOW ON A SOLID SPHERE WITH NEWTONIAN HEATING," *Acta Applicandae Mathematicae*, vol. 112, no. 3, pp. 263-274, 2010, doi: https://doi.org/10.1007/s10440-010-9567-5.

[20] M. Salleh, R. Nazar, and I. Pop, "MIXED CONVECTION BOUNDARY LAYER FLOW ABOUT A SOLID SPHERE WITH NEWTONIAN HEATING," *Archives of Mechanics*, vol. 62, no. 4, pp. 283-303, 2010. https://doi.org/10.3814/2010/736039

[21] R. Mahat, S. Shafie, and I. Ullah, "FREE CONVECTION OF VISCOELASTIC NANOFLUID FLOW ON A HORIZONTAL CIRCULAR CYLINDER WITH CONSTANT HEAT FLUX," *Journal of Advanced Research in Applied Sciences and Engineering Technology*, vol. 30, no. 3, pp. 1-8, 2023, doi: https://doi.org/10.37934/araset.30.3.18.

[22] R. Mahat, M. Saqib, I. Ulah, S. Shafie, and S. M. Isa, "MHD MIXED CONVECTION OF VISCOELASTIC NANOFLUID FLOW DUE TO CONSTANT HEAT FLUX," *Journal of Advanced Research in Numerical Heat Transfer*, vol. 9, no. 1, pp. 19-25, 2024.

[23] F. A. Alwawi, H. T. Alkasasbeh, A. M. Rashad, and R. Idris, "NATURAL CONVECTION FLOW OF SODIUM ALGINATE BASED CASSON NANOFLUID ABOUT A SOLID SPHERE IN THE PRESENCE OF A MAGNETIC FIELD WITH CONSTANT SURFACE HEAT FLUX," *in Journal of Physics: Conference Series*, 13-25 July, 2019.doi:https://doi.org/10.1088/1742-6596/1366/1/012005.

[24] F. A. Alwawi, A. S. Hamarsheh, H. T. Alkasasbeh, and R. Idris, "MIXED CONVECTION FLOW OF MAGNETIZED CASSON NANOFLUID OVER A CYLINDRICAL SURFACE," *Coatings*, vol. 12, no. 3, p. 296, 2022, doi: https://doi.org/10.3390/coatings12030296.

[25] L. A. Aziz, A. R. M. Kasim, M. Z. Salleh, and S. Shafie, "MIXED CONVECTION BOUNDARY LAYER FLOW ON A SOLID SPHERE IN A VISCOELASTIC MICROPOLAR FLUID," *in Proceedings of the Third International Conference on Computing, Mathematics and Statistics (iCMS2017)* pp. 111-117. doi:https://doi.org/10.1007/978-981-13-7279-7_14.

[26] A. C. Eringen, "THEORY OF MICROPOLAR FLUIDS," *Journal of mathematics and Mechanics*, pp. 1-18, 1966. https://doi.org/10.1512/iumj.1967.16.16001

[27] T. Chen and A. Mucoglu, "ANALYSIS OF MIXED FORCED AND FREE CONVECTION ABOUT A SPHERE," *International Journal of Heat and Mass Transfer*, vol. 20, no. 8, pp. 867-875, 1977. doi: https://doi.org/10.1016/0017-9310(77)90116-8

[28] R. Nazar and N. Amin, "FREE CONVECTION BOUNDARY LAYER ON AN ISOTHERMAL SPHERE IN A MICROPOLAR FLUID," *International Communications in Heat and Mass Transfer*, vol. 29, no. 3, pp. 377-386, 2002, doi: https://doi.org/10.1016/S0735-1933(02)00327-5.

[29] R. Nazar, N. Amin, and I. Pop, "MIXED CONVECTION BOUNDARY LAYER FLOW ABOUT AN ISOTHERMAL SPHERE IN A MICROPOLAR FLUID," *International Journal of Thermal Sciences*, vol. 42, no. 3, pp. 283-293, 2003, doi: https://doi.org/10.1016/S1290-0729(02)00027-3.

[30] L. A. Aziz, A. R. M. Kasim, M. Z. Salleh, N. S. Yusoff, and S. Shafie, "MAGNETOHYDRODYNAMICS EFFECT ON CONVECTIVE BOUNDARY LAYER FLOW AND HEAT TRANSFER OF VISCOELASTIC MICROPOLAR FLUID PAST A SPHERE," *in Journal of Physics: Conference Series*, p. 012003.doi:https://doi.org/10.1088/1742-6596/890/1/012003.

[31] N. S. Khashi'ie, N. Arifin, E. H. Hafidzuddin, and N. Wahi, "MHD MIXED CONVECTIVE STAGNATION POINT FLOW WITH HEAT GENERATION PAST A SHRINKING SHEET," *ASM Sci. J*, pp. 71-81, 2019.

[32] H. A. Nabwey, A. M. Rashad, A. M. EL-Hakiem, and S. I. Alshber, "EFFECTIVENESS OF NEWTONIAN HEATING ON MAGNETO-FREE CONVECTIVE FLOW OF POLAR NANOFLUID ACROSS A SOLID SPHERE," *Fractal and Fractional*, vol. 6, no. 2, p. 57, 2022, doi: https://doi.org/10.3390/fractalfract6020057.

[33] M. K. A. Mohamed, N. M. Sarif, N. Noar, M. Z. Salleh, and A. Ishak, "VISCOUS DISSIPATION EFFECT ON THE MIXED CONVECTION BOUNDARY LAYER FLOW TOWARDS SOLID SPHERE," *Trans. Sci. Technol*, vol. 3, no. 1-2, pp. 59-67, 2016.

[34] S. H. M. Yasin, M. K. A. Mohamed, Z. Ismail, B. Widodo, and M. Z. Salleh, "NUMERICAL INVESTIGATION OF FERROFLUID FLOW AT LOWER STAGNATION POINT OVER A SOLID SPHERE USING KELLER-BOX METHOD," *Journal of Advanced Research in Fluid Mechanics and Thermal Sciences*, vol. 94, no. 2, pp. 200-214, 2022, doi: https://doi.org/10.37934/arfmts.94.2.200214.